Electronic Supplementary Material (ESI) for Analyst.

Supporting Information

A chitosan-Au-hyperbranched polyester nanoparticles-based antifouling immunosensor for sensitive detection of carcinoembryonic antigen

Chong Sun[a,b], Lie Ma[a], Qiuhui Qian[a], Soniya Parmar[c], Wenbo Zhao*[,a], Bo Zhao[a], Jian Shen*[,a]

[a]*Jiangsu Collaborative Innovation Center of Biomedical Functional Materials, Jiangsu Key Laboratory of Biofunctional Materials,College of Chemistry and Materials Science, Nanjing Normal University, Nanjing 210023, PR China*

[b]*Key Laboratory for Soft Chemistry and Functional Materials of Ministry of Education, School of Chemical Engineering, Nanjing University of Science and Technology, Nanjing 210094, PR China*

[c]*Department of Biological Sciences and Bioengineering, Indian Institute of Technology, Kanpur 208016, India*

*Corresponding authors.

E-mail address: zhaowenbo@njnu.edu.cn, jshen@njnu.edu.cn.

Tel/Fax: +862583598280.

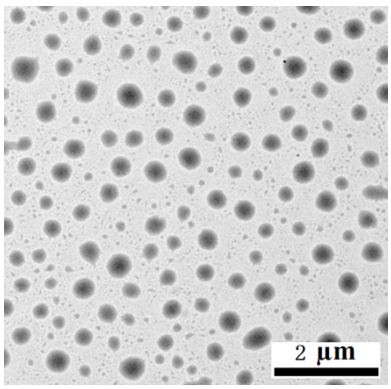

Fig. S1. Representative TEM for HBPE-CA NPs.

Clinically, activated partial thromboplastin time (APTT), prothrombin time (PT) and thrombin time (TT) are used to evaluate *in vitro* the antithrombogenicity of a given biomaterial.[1,2] The results were given in Fig. S2. There was no significant difference of TT values between the control sample (12.3 s) and HBPE-CA NPs (12.2 s). But the APTT/PT were statistically longer in test (25.1 s/13.9 s) after the injection of HBPE-CA NPs than in controls (22.0 s/9.8 s), respectively. Thus, it is considered that the good antithrombogenicity of HBPE-CA NPs can be attribute to the surface modification of HBPE with carboxylic acid functional groups that produce electrostatic repulsion between the material surface and blood components.[3]

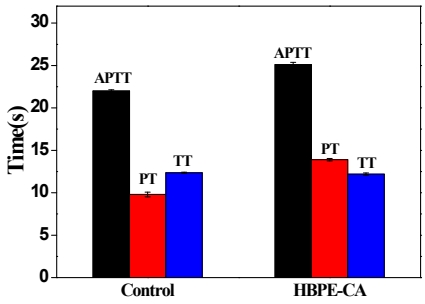

Fig. S2. Coagulation assays of HBPE-CA NPs.

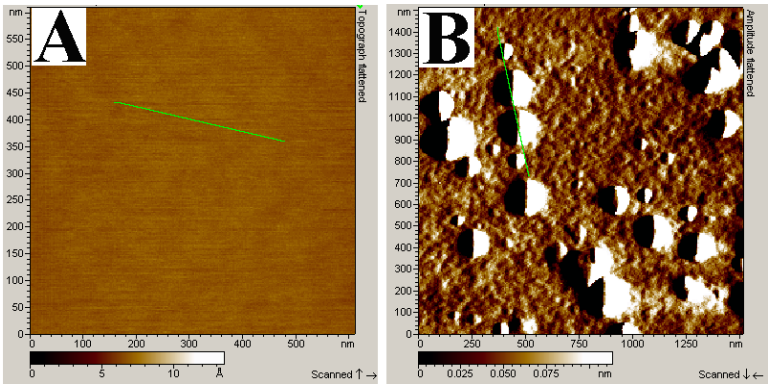

Fig. S3. The AFM images of (A) blank GCE, and (B) GCE electro-deposited with CS-Au NPs.

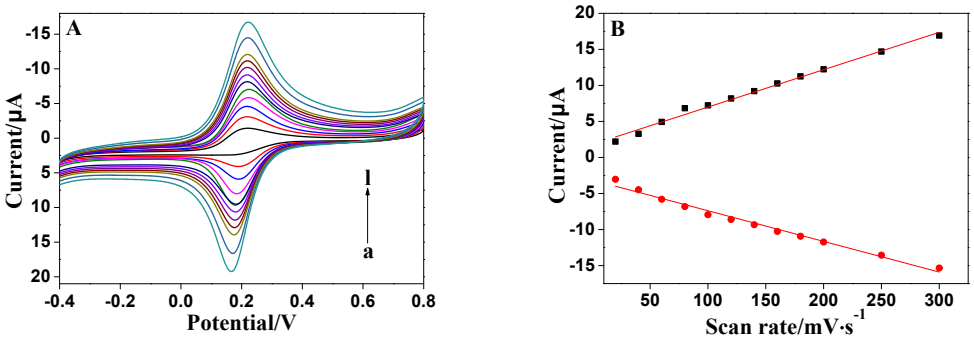

Fig. S4. (A) CVs of (HBPE-CA)/CS-Au modified GCE in 0.1 M PBS (pH=7.4) at different scan rates. Scan rate (from a to l): 20, 40, 60, 80, 100, 120, 140, 160, 180, 200, 250, 300 $mV \cdot s^{-1}$. (B) Plots of anodic and cathodic peak current vs. scan rate.

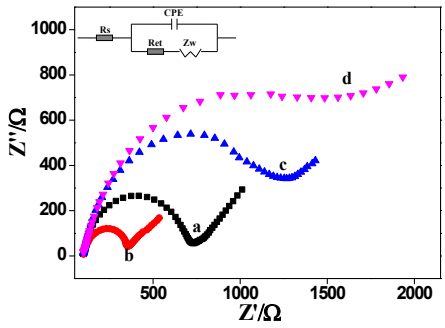

Fig. S5. Electrochemical impedance spectra of (a) bare GCE, (b) CS-Au/GCE, (c) (HBPE-CA)/CS-Au/GCE and (d) anti-CEA/(HBPE-CA)/CS-Au/GCE recorded at the open circuit potential in 10 mM $[Fe(CN)_6]^{3-/4-}$(1:1) solution containing 0.1 M KCl. Inset is a schematic of the equivalent circuit.

Table S1. Comparison of analytical properties of some electrochemical immunosensors towards CEA.

Electrochemical immunosensors	Detection limit ($fg \cdot mL^{-1}$)	Linear range ($fg \cdot mL^{-1}$)	Ref.

Anti-CEA/HRP/magnetic gold	1×10^4	1×10^4-1.6×10^8	Tang et al., 2008
Anti-CEA/AuNPs/PB	1.4×10^3	2.5×10^2-2×10^6	Lai et al., 2009
Anti-CEA/AuNP/TH/NF	5×10^3	1×10^4-1.2×10^7	Lia et al., 2011
BSA/anti-CEA/nano-Au/PDDA	1.6×10^4	5×10^4-4.5×10^7	Liang et al., 2011
Anti-CEA/Au-Gra/CS-Fc+TiO_2	3.4×10^3	1×10^4-8×10^7	Han et al., 2011
Anti-CEA/AuNPs@nafion/Fc@CHIT	3×10^3	1×10^4-1.5×10^8	Shi and Ma, 2011
Anti-CEA/Ag-SiO_2@nafion/Thi@CHIT	1	1-1×10^5	Wang et al., 2013
Anti-CEA/(HBPE-CA)/CS-Au/GCE	0.251	1-1×10^7	This work

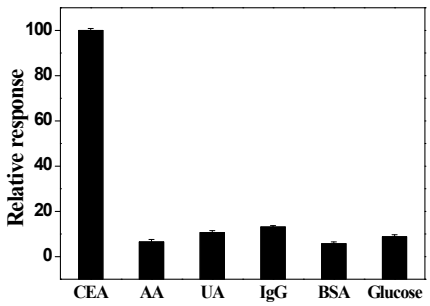

Fig. S6. The selectivity of the developed immunosensor for CEA.

References:

1 F.Y. Du, H. Wang, W. Zhao, D. Li, D.L. Kong, J. Yang and Y.Y. Zhang, *Biomaterials,* 2012, **33**, 762-770.

2 S.E. Skrabalak, J. Chen, L. Au, X. Lu, X. Li and Y.N. Xia, *Adv. Mater.,* 2007, **19**, 3177-3184.

3 K. Yu and J.N. Kizhakkedathu, *ACS Symp. Ser.,* 2012, **1120**, 577-603.